

Electrochemical and Gravimetric Study on Corrosion Inhibition of Carbon Steels Exposed to Oilfield Produced Water

L. M. Quej-Ake*, J. L. Alamilla, A. Contreras

Instituto Mexicano del Petróleo, Eje Central Lázaro Cárdenas Norte 152, Col. San Bartolo Atepehuacan, 07730, Ciudad de México, México.

*Corresponding author: L. M. Quej-Ake, email: lquej@imp.mx

Received December 27th, 2022; Accepted May 5th, 2023.

DOI: <http://dx.doi.org/10.29356/jmcs.v67i4.1937>

I dedicate this work to emeritus SNI researchers for their outstanding contributions to electrochemical science.

Abstract. Two corrosion inhibitors (CI) were evaluated to study the protection behaviours of three carbon steels: X52, X60, and X70 in an oilfield produced water. The water was subjected to unstirred condition and a rotation speed of 600 rpm to simulate a stagnant and homogeneous solutions, respectively, it is in pipelines at temperature range of 30 °C to 60 °C. The internal corrosion rate and inhibition efficiencies were measured using polarization curves and gravimetric tests, complimented with the surface analysis of the corroded carbon steel samples using scanning electron microscopy (SEM). The experimental results suggested that the chlorides compounds, H₂S, metals, and the inhibitor type modified the corrosion rate of the carbon steels under study. High corrosion rates were achieved on X70 steel at the temperature of 30 °C and 50 °C under 600 rpm. It was determined that X52 steel had the highest corrosion rate at 60 °C and 600 rpm. While an adequate protection of X70 steel was confirmed with a high inhibition efficiency using a naphthenic imidazoline as corrosion inhibitor.

Keywords: Inhibitor; pipeline steel; protection; storage tanks.

Resumen. Se evaluaron dos inhibidores de corrosión para estudiar los comportamientos de protección de tres aceros al carbono: X52, X60 y X70 en agua congénita. El agua se sometió a condiciones sin agitación y una velocidad de rotación de 600 rpm para simular soluciones estancadas y homogéneas, respectivamente, el cual se encuentra en tanques de almacenamiento y tuberías en un rango de temperatura de 30 °C a 60 °C. La velocidad de corrosión interna y los valores de las eficiencias a la inhibición se determinaron mediante curvas de polarización y pruebas gravimétricas, las que fueron complementadas con el análisis de la superficie de las muestras de acero al carbono corroídas mediante microscopía electrónica de barrido. Los resultados experimentales sugirieron que los compuestos de cloruros, H₂S, metales y el tipo de inhibidor, modificaron la velocidad de corrosión de los aceros al carbono en estudio. Altos valores de corrosión en acero X70 fueron alcanzados a la temperatura de 30 °C y 50 °C usando 600 rpm. Se determinó que el acero X52 tuvo la velocidad de corrosión más alta a 60 °C y 600 rpm. Mientras que se confirmó una protección adecuada del acero X70 con una alta eficiencia de inhibición usando imidazolina nafténica como inhibidor de corrosión.

Palabras clave: Inhibidor; acero de ducto; protección; tanques de almacenamiento.

Introduction

The operating tanks and oil pipelines are subjected to internal corrosion problems during the storage and transmission of crude oil [1-3]. They are protected against oilfield produced water (OPW) containing corrosive substances by using corrosion inhibitors [3-7]. However, the internal corrosion problems are increased when this type of water is subjected to flowing media and operating temperatures, where the solution have been stirred or displacing during the entire time of exposure of the operating process or laboratory experiments. As a result, the internal damage is affected by different corrosive and toxic compounds such as dissolved gases such as chlorides, hydrogen (H₂), hydrogen sulfide (H₂S), carbon dioxide (CO₂), naphthenic acid, resins, high asphaltene contents, water with high concentrations of salts and their associated ions [8-13]. There are serious problems with the oilfield data to mitigate the corrosion rate because the halides other than chlorides are not addressed, and the corrosion knowledge requires major improvements. Moreover, internal corrosion is caused by changes in environments where the combined interactions between the corrosive compounds hydrodynamic and temperature dependence occurs, resulting in localized and generalized losses of wall thickness attributed to local or general of mass loss of a metal [14,15]. Thus, the electroactive environments and impurities contained in the OPW could activate the minimum amount of energy to starts the corrosion reaction modifying the oxides, passive films, and the rate of deterioration on a specific metal exposed to chloride compounds [16-18]. The type of localized or generalized corrosion that starts will depend on the type and its metallography of the American Petroleum Institute (API) steel grades [19-22]. However, in field practices, the internal corrosion rate measurement is obtained from a commercial and nonindustrial corrosion coupon such as SAE 1018 steel. The inhibition of an API pipeline steel using low concentrations of an organic molecule is the ability of active agent adsorption (inhibitor) to donate electrons on active-susceptible sites (anodic sites) and thus to avoid the mass loss such as Fe²⁺ or Fe³⁺ from them [20,22,23]. In this way, the steel surface can gain electrons, the source of energy required by an electrochemical process to start the inhibition. The electrochemical tests are versatile tools where cathodic-anodic processes related to open circuit potential can take place, with particular importance on polarization curves [24]. This type of technique must be used as a procedure in which the reduction and oxidation process of an inhibitor is able to study and determine if the organic molecule can act as a cathodic, an anodic (donor), or mixed corrosion inhibitor by using a forced energy with particular importance on the cathodic and anodic slopes determined from Tafel region. It can be complemented by using gravimetric measurement to understand the natural rate of deterioration of metals. In this work, the internal corrosion process and mitigation study of three API steels immersed in a Mexican OPW under stagnant (0 rpm) and dynamic (600 rpm) conditions, and the temperature range of 30 °C to 60 °C was highlighted. The aim of the stagnant or unstirred condition was to simulate the internal corrosion under a static situation, where the hydrocarbon containing water phase and corrosion inhibitor is stored in a tank or a pipeline. The inhibition study of the API grade steels exposed to an OPW was conferred. CR values of these steels immersed in OPW were obtained by using Tafel parameters and weight loss. X70 steel immersed in OPW was apparently less corroded than those for the API steels evaluated under 600 rpm and 60 °C. The naphthenic imidazoline corrosion inhibition decreased the current densities based on to the cathodic and anodic perturbation.

Experimental

Sample used

Table 1 shows the ions and metals determined in a Mexican OPW, which was collected (twenty liters) in a storage tank of a crude oil production in Mexico. Ion chromatography and inductively coupled plasma optical emission spectrometry were applied to identify the ions and metals within the OPW. A Perkin-Elmer optima 7300 DV device and EPA 6010C method were applied for the metal identifications [25]. A Dionex DX500 equipment and ASTM D 4327-03 test method were applied for measured the ions within the OPW [26].

Table 1. Fundamental ions identified in a Mexican OPW in mg/L.

Na ⁺	Ba ⁺	Ca ²⁺	Mg ²⁺	Cl ⁻	HCO ₃ ⁻	CO ₃ ²⁻	SO ₄ ²⁻	H ₂ S	CO ₂	N ₂
14,250	241	47,530	5,300	43,905	399	110	445	740	39,560	8,550

Inhibitor used

A concentration of 50 mg/L of an imidazoline derivative (CI-1: CH₂-CH₂-N=C-R₂-N-CH₂-CH₂-R₁; R₁ is an alkyl radical containing a CH₂ chain around 12 to 16 carbons) and a naphthenic imidazoline (CI-2: CH₂-CH₂-N=C-R₂-N-CH₂-CH₂-O-CH₂-CH₂-N-CH₂-CH₂-N=C-R₂; R₂ contains CH₂-CH₂-CH₂-CH₂-CH(R₁)) corrosion inhibitor was used to study the corrosion mitigation of three carbon steels exposed to OPW under flowing media and temperature [27,28].

Electrochemical cell used

A conventional electrochemical cell with a volume of 100 mL coupled with a recirculation bath (Thermomix 1460) to control the temperature in the range of 30 °C to 60 °C ± 0.05 °C was used. The working electrodes were made of three API pipeline steels with an exposure area of 0.5 cm² (previously mechanically polished with a series of emery paper from 240 up to grade 600 and then cleaned in an ultrasonic bath with acetone for 1 min). The auxiliary electrode was a platinum rod, and the reference was a saturated calomel electrode (SCE). The chemical composition and mechanical properties for the three API steels have been documented earlier [19,29].

Electrochemical characterization

The polarization curves were applied after 1 h of open circuit potential (OCP). During the polarization, a volume flow rate of 10 mL per minute of nitrogen gas per 100 mL of test solution was continuously aerated until reach around 5 parts per billion of oxygen in the OPW as was recommended by several standard test procedures (ASTM G170, ASTM G184, ASTM G185, and NACE TM0177) [30-33]. A rotational speed of 600 rpm using a rotating disk electrode was used to achieve a homogeneous OPW to obtain good current density responses [34]. A Potentiostat/Galvanostat Solartron SI 1287 coupled with a personal computer was used to obtain the electrochemical data, where a potential scan of ± 250 mV with respect to OCP, and a scanning rate potential of 0.166 mV/s were performed. The value of the corrosion current density (*i*_{corr}) was obtained by the graphical intersection procedure using a Tafel range of ± 120 mV from the corrosion potential (*E*_{corr}). It was used for the general or forced corrosion rate (CR) analysis of the carbon steels exposed to OPW. Thus, CR was calculated from the procedure recommended by ASTM G102 that concern the equations (1) and (2) [35]:

$$CR(mm/year) = \frac{i_{corr}W}{nF\rho} \quad (1)$$

$$CR(mils.per.year:mpy) = \frac{i_{corr}EW0.13}{A\rho} \quad (2)$$

where W is the atomic weight of the metal; n is the number of the electrons participating in the electrochemical reaction; F is the Faraday constant (96500 C or 96500 amp.sec); ρ is the density of the metal in g/cm; EW is the equivalent weight of the metal; and A is the exposure area in cm².

Inhibition efficiency

The inhibition efficiency (IE, %) of the two CIs was calculated using the following equation (3) [36]:

$$IE, \% = \frac{CR - CR_{inh}}{CR} 100 \quad (3)$$

where, CR and CR_{inh} are the corrosion rate in the absence and presence of an inhibitor, respectively.

Analysis of the CR using the Arrhenius equation

The linearization of the Arrhenius law from the temperature range of 30 , 40, 50 and 60 °C was analysed by CR profiles by the following equation (4) to determine the activation energies (E_a) of corrosion of the three API steels [36].

$$\ln CR = \left(\frac{-E_a}{R}\right)\left(\frac{1}{T}\right) + \ln A \quad (4)$$

where R is the molar gas constant in J/mol°K, T is the absolute temperature in °K, A is a pre-exponential factor or frequency factor for the collisions between the active molecules and the active sites on the metal surface where susceptible areas such as pearlite (anodic site) and ferrite (cathodic site) for low carbon steels might happen [19-21].

Gravimetric procedure

Twelve beakers of 60 mL of the total volume containing 50 mL of OPW and each API steel were used to carry out the gravimetric test. They were covered with a hermetic seal to minimize the solution loss through evaporation and maintaining them at room temperature during 30 days of exposure time. All experimental test solutions were subjected to unstirred condition to simulate a stagnant condition in a storage tank or pipeline. Before the gravimetric test, all API steel samples were mechanically polished with emery paper up to grade 600, and then were cleaned in an ultrasonic bath with acetone for 1 min. Then, the initial weight of each steel sample was measured. Thus, cylinders and cuboids of the three steels were suspended into each beaker with the OPW by using a thread, where the cylindrical geometry of each steel was exposed to OPW only and cuboid of each steel was exposed to OPW containing 50 mg/L CI-2 added. Duplication of the gravimetric data to justify the repeatability were taken into consideration in the experimental design. Based on the weight loss tests, natural CR values that involve the weight loss for each carbon steel were determined by using the following equation (5) [37]:

$$CR = \frac{(\text{Initial. Weight} - \text{Final. Weight})k}{Apt} \quad (5)$$

where k is the unit factor (365,000 for mm/year and 22,300 for mils per year: mpy); A is the area of exposure in mm² for mm/year and inches squared (in²) for mpy; and t is the exposure time of the metal with the corrosive environment in days (d).

Surfaces cleaning procedure

To remove the corrosion products on the corroded API steel surfaces in accordance with ASTM G1 and NACE/ASTM TM0169 [38,39], and to observe the finished surface after experiment, an inhibited hydrochloric acid (HCl) solution containing a mixture of 1000 mL of concentrated HCl + 50 g/L stannous chloride (SnCl₂) + 20 g/L antimony trioxide (SbO₃) was prepared. Thus, a volume of 100 mL of various chemical substances was sequentially used to clean each corroded steel: (1) chloroform, (2) acetone, (3) deionized water, (4) inhibited HCl, and (5) 5 wt.% of bicarbonate; later, each steel was cleaned with a brush and deionized water and finally dried and weighed out (final weight).

Scanning electron microscopy

The physical features of the more damaged steel surface and its corrosion products were obtained by scanning electron microscopy (SEM) using a Phillips ESEM-XL30 equipped with an EDAX.

Results and discussion

Physicochemical features of the oilfield produced water

Table 1 shows the quantity of ions identified in a Mexican OPW. It was confirmed that the OPW had a high amount of chloride elements and several types of metals and carbonates in the form of soluble salts. The mixtures of high concentrations of halides other than chlorides and H_2S could be led to a localized attack on internal pipeline walls by acid sour saltwater medium where a possible pitting initiation might occur [40-42]. They play a dominant role in determining an internal aqueous attack problem on pipe steels exposed to a salty and acidic sour solution or acid sour saltwater.

Polarization curves

Fig. 1 shows the polarization curves recorded for three API steels exposed to OPW at stagnant conditions, temperature dependence, and after 1 h of exposure time. The positive polarization referred to OCP is a form of metallic oxidation, where an anodically electrified interface (well-behaved electrified anode) is reached based on the electrochemical property (anodic current density obtained as a response) of each API steel in direct contact with the acid sour saltwater subjected to the action of an unstirred condition. The contribution of the oxidation on API steel surface is increased when temperature was shifts from 30 °C to 60 °C. On the other hand, when the contribution of the reduction takes place, the polarization is displacing toward negative potentials where a well-behaved electrified cathode is reached. This forced corrosion is attributed to the formation of a cathode or cathodic area if the exposed area of the steel is impressed a cathodic current density (free electron flow). A contrary effect is carried out if the exposed area of the steel is removed the electrons where an anode (anodic area) is expected. This is a well-behaved cathode or well-behaved anode, where a reduction-oxidation processes is taken into consideration. Thus, the steel/OPW interfaces were electrically forced to reach more negative charges converting them into a cathodically electrified interface based on the electrochemical properties of each API steel, corrosive solution, and temperature dependence. Additionally, a cathodic peak related to the reduction process on X60 steel under 30 °C and 40 °C was acquired, which means that a possible incrustation or calcareous deposit was obtained [43].

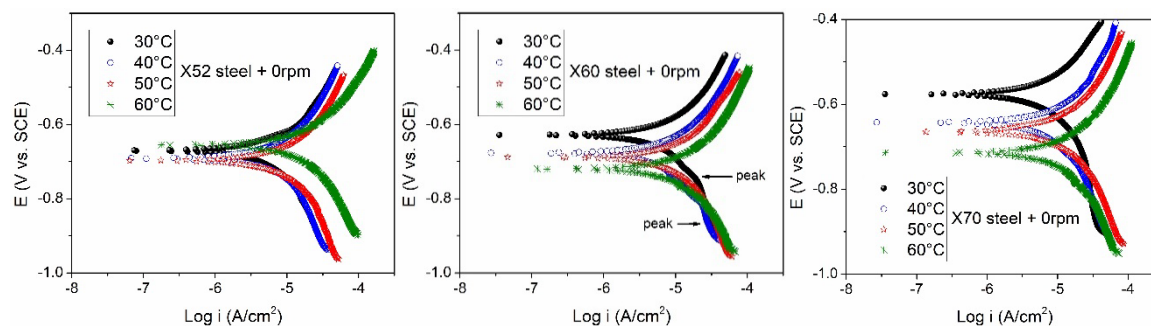


Fig. 1. Polarization curves for three steels exposed to OPW at stagnant condition (0 rpm) showing the temperature dependence after 1 hr of exposure.

Fig. 2 shows that the hydrodynamic condition increased the current density responses, but the modification of the current densities depended on the type of API steel and the temperature dependence. Moreover, the corrosion potentials recorded in each type of steel were displacing toward more negative values, which is attributed to a higher susceptibility to oxidation trends [44]. Acquired Tafel polarization range of three steels exposed to OPW at stagnant condition and 600 rpm, temperature dependence, and 1 h of exposure time are shown in Tables 2 and 3, respectively [35]. CR were determined to be studied the forced corrosion rate by using electrochemical testing [24]. Regarding the Table 2, it is possible to observe that X60 steel was more susceptible to corrosion process when it was subjected to stagnant condition at 30 °C, 50 °C, and 60 °C. Moreover, a minor corrosion rate on X52 steel at 30 °C was obtained. Acquired Tafel parameters at 600 rpm

(Table 3) indicated that the rate of deterioration was increased as a function of the carbon steel grades and temperature in comparison with stagnant condition. However, this effect is only observed at 30 °C and 50 °C. Because random corrosion rates were reached at the rest of temperatures in both hydrodynamic systems, and a major susceptibility to corrosion on X52 steel at 600 rpm and 60 °C was obtained. The random corrosion rate of each electrochemical system corroborates the difficult and complex susceptibility to corrosion on API steels exposed to OPW under hydrodynamic condition and temperatures. Perhaps, the halides, sulfides, and CO₂ compounds within the OPW, in the form of a so salty and acidic sour solution, could made mixtures of more corrosive contaminants when they are subjected to hydrodynamic situations and temperatures. Therefore, each type of OPW could contain different types of corrosive contaminants in which their physicochemical properties are always in random changes due to the geographical area of the oilfield well. According to the qualitative categorization of API steel CRs for oil pipelines documented by the NACE Standard SP0775 [37], the corrosion damage related to the three steels exposed to OPW is very severe because their CR values were higher than 0.25 mm/year, where X52 steel had the highest values of CR at 600 rpm and 60 °C.

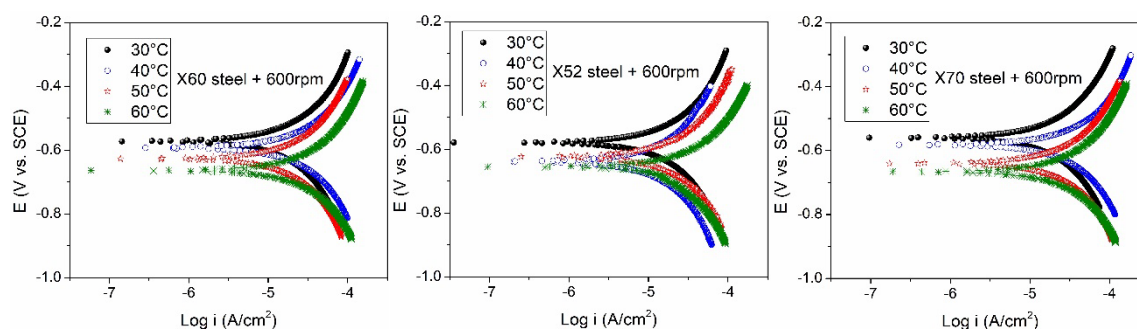


Fig. 2. Polarization curves for three steels exposed to OPW at 600 rpm showing the temperature dependence after 1 hr of exposure.

Table 2. Tafel polarization data of three steels exposed to OPW at stagnant condition showing the temperature dependence after 1 hr of exposure time.

Steel	E_{corr} (mV/SCE)	β_a (mV/dec)	$-\beta_c$ (mV/dec)	i_{corr} (A/cm ²) $\times 10^{-5}$	CR	
					(mm/year)	(mpy)
30 °C						
X52	-670	329	588	1.5329	0.18	6.93
X60	-628	399	540	2.2969	0.27	10.39
X70	-575	340	695	2.1254	0.25	9.61
40 °C						
X52	-691	522	630	2.3538	0.27	10.64
X60	-676	325	285	2.6506	0.31	11.99
X70	-643	340	695	2.8988	0.34	13.11
50 °C						
X52	-697	435	642	2.4742	0.28	11.18
X60	-688	496	258	3.4840	0.40	15.76
X70	-664	346	384	2.7740	0.32	12.54
60 °C						
X52	-655	330	540	3.5069	0.41	15.85
X60	-720	375	578	3.9190	0.45	17.72
X70	-714	382	780	3.5123	0.40	15.88

Table 3. Tafel polarization data of three steels exposed to OPW at 600 rpm showing the temperature dependence after 1 hr of exposure time.

Steel	E_{corr} (mV/SCE)	β_a (mV/dec)	$-\beta_c$ (mV/dec)	i_{corr} (A/cm ²) $\times 10^{-5}$	CR	
					(mm/year)	(mpy)
30 °C						
X52	-578	470	482	2.4716	0.28	11.17
X60	-572	395	509	3.0518	0.35	13.80
X70	-560	322	356	3.2621	0.37	14.75
40 °C						
X52	-623	432	533	3.0243	0.35	13.67
X60	-592	473	532	3.9929	0.46	18.05
X70	-582	470	509	3.6559	0.42	16.53
50 °C						
X52	-622	471	505	3.9409	0.45	17.82
X60	-626	456	493	4.6975	0.54	21.24
X70	-640	365	502	5.3322	0.61	24.11
60 °C						
X52	-654	362	243	6.4633	0.74	29.22
X60	-663	479	508	5.6325	0.65	25.47
X70	-665	460	484	5.6381	0.65	25.49

The effect of temperature

Fig. 3 shows the CR profiles as a function of the temperature of the X52, X60, and X70 steels immersed in OPW where the solutions have been unstirred and stirred during the entire time of experiment using 0 rpm and 600 rpm (flowing media), and Table 4 shows the acquired E_a range. It is important to mention that the data acquired from the X52 steel indicated the presence of a nonlinear profile, where minor CR values corresponded to high activation energies in the range of 17.0 kJ/mol to 27.7 kJ/mol under flowing media, which were determined from the slopes. When the CR is involved in the activation energy, then the following analysis is taken into consideration [13,43,45-47]:

When CR is high, then E_a is low; thus, a chemisorption is considered.

When CR is low, then E_a is high; thus, a physisorption is considered.

This is indicative to a profound impact on the internal corrosion on X60 and X70 steels exposed to OPW so salty and acidic sour solution because a minimum quantity of E_a should be required to start a rate of the steel dissolution as a result of an initial electrochemical deterioration [45-47]. It was reported that the result of E_a obtained from X65 steel exposed to acidic solution was around 21.08 kJ/mol [48]. There are, average of E_a values determined from the slopes: E_a about 28.46 kJ/mol to 54.35 kJ/mol, E_a about 16.68 kJ/mol to 34.31 kJ/mol, and E_a around 20 kJ/mol when carbon steel was exposed to 0.5 M HCl containing inhibitors, cooling water containing inhibitors, and 1 % NaCl containing CO₂, respectively [49-51]. It is important to mention that these results of E_a values were obtained under temperatures in the range of 35 °C to 80 °C using weight loss and electrochemical methods as well [49-51]. As the temperature dependence had the most drastic condition on corrosion initiation, it is assumed that inhibitor can act as organic barrier for internal corrosion at 600 rpm, 1 h, and 60 °C.

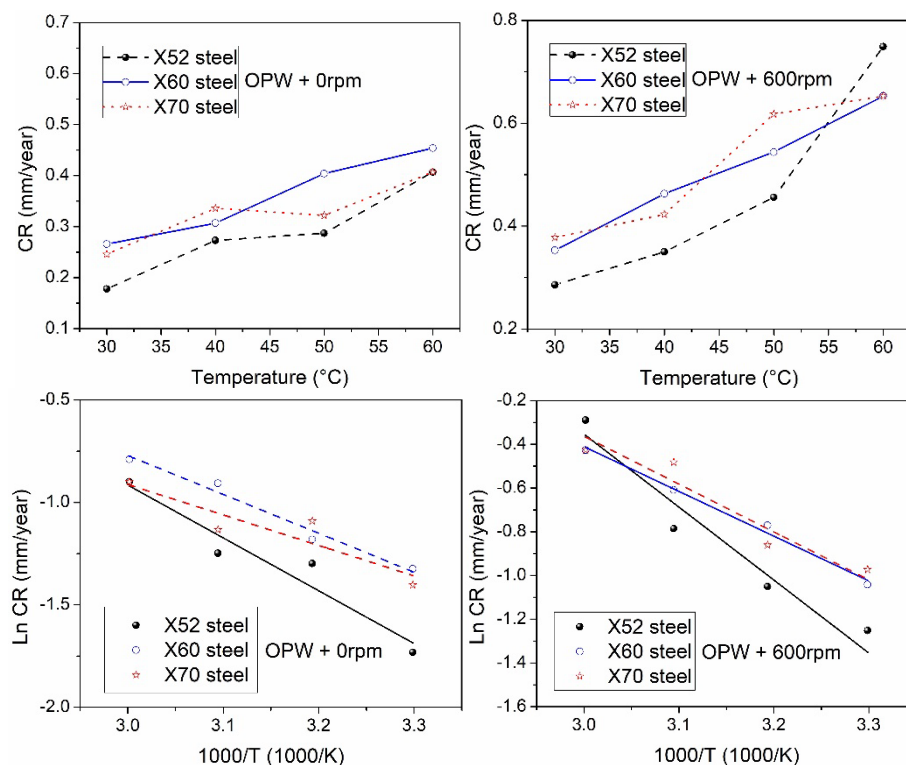


Fig. 3. Temperature effect on CR at 0 and 600 rpm, and Arrhenius plots for steels exposed to OPW at stagnant condition, 600 rpm, and after 1 h of exposure time.

Table 4. Activation energy values determined from polarization data of three carbon steels exposed to OPW at 0 rpm, 600 rpm, and after 1 h of exposure time.

Steel	Adj. R-Square (R ²)	-E _a (kJ/mol)	Adj. R-Square (R ²)	-E _a (kJ/mol)
	0 rpm		600 rpm	
X52	0.93	21.4	0.94	27.7
X60	0.97	15.7	0.99	17.0
X70	0.83	12.3	0.92	18.1

Corrosion inhibition

Fig. 4 shows the polarization curves of the three API steels exposed to OPW in the presence of 50 mg/L of CI-1 and CI-2 subjected to 600 rpm, 1 h, and 60 °C, and Table 5 shows the acquired Tafel polarization data. It is important to note that the corrosion potentials were displacing toward positive values with particular interest on X60 and X70 steels. Apparently, a minor corrosion current density response on X70 steel was recorded in CI-2 than those of the same steel in CI-1 and OPW in the absence of an inhibitor. This result is supported by the NACE Standard SP0775 [37], where a low corrosion rate categorization of X70 steel for oil environments is proposed. Thus, the corrosion rate was mitigated as a consequence of the CI-2, corroborating that this type of steel corresponded to an IE of 97.2 %. The IE value of this feature suggests the presence of electron donors, what suggest inhibitors species were adsorbed in the active sites and a greater surface coverage (surface adsorption of the inhibitive molecules) is preserved. Moreover, the increase of the corrosion current densities on the three steels in the presence of the CI-1 is attributed to the short chain organic molecules as corrosion inhibitor (inhibitor used). This type of inhibitor is designed to internal corrosion control in oil and gas pipelines containing mixtures of H₂S

and CO₂ which are highly corrosive agents to steel [27,28]. CI-2 has long chain organic molecules, and it is designed to corrosion control in oil and gas pipes containing mixtures of oil-in-water emulsions containing high volume of OPW [52].

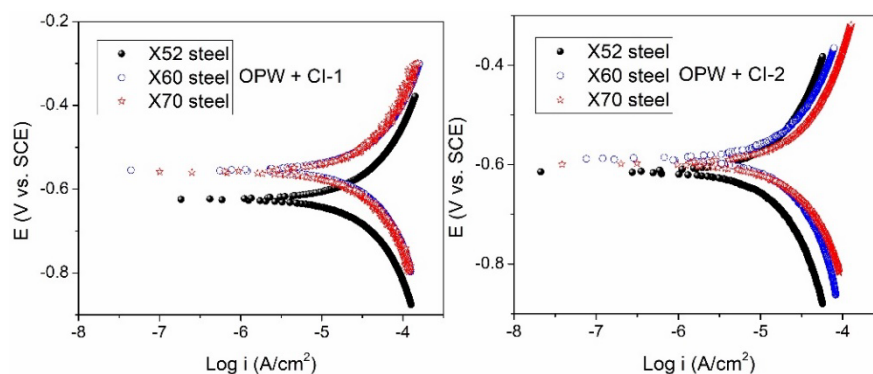


Fig. 4. Polarization curves of steels in OPW containing 50 mg/L of CI-1 and CI-2 at 60°C, 600 rpm, and after 1 h of exposure time.

Table 5. Tafel polarization data of three steels exposed to OPW containing 50 mg/L of CI-1 and CI-2 at 60 °C, 600 rpm, and after 1 h of exposure time.

Steel	E_{corr} (mV/SCE)	β_a (mV/dec)	$-\beta_c$ (mV/dec)	i_{corr} (A/cm ²) $\times 10^{-5}$	CR		IE (%)
					(mm/year)	(mpy)	
CI-1							
X52	-624	120	129	5.5432	0.64	25.068	14.1
X60	-554	97	111	6.5380	0.75	29.567	-
X70	-558	125	125	5.1761	0.60	23.408	8.1
CI-2							
X52	-614	243	278	2.4657	0.28	11.15	61.9
X60	-588	77	83	2.2446	0.26	10.15	60.1
X70	-598	82	82	0.1598	0.02	0.72	97.2

Gravimetric measurement

Table 6 shows the CR and IE values of X52, X60, and X70 steels exposed to OPW. These parameters were determined to be studied the natural corrosion rate by means duplicated weight loss evaluations following in unstirred (stagnant) CI-2. The CR value in each steel was lower than those of the same steel determined by an applied anodic and cathodic polarization (Table 5). The determined IE value was a consequence of its natural and low corrosion rate reaching a maximum value for X70 steel, but it was evidence of a poor surface adsorption of the inhibitive molecule reaching a lower surface coverage. Perhaps, the OPW sample containing CI-2 must be stirred during the entire time of experiment. As a result, the obtained IE (fraction of the covered area) had a lower value and still it does not seem to be well understood and compared with results determined under a forced energy and 600 rpm (Table 5). It demonstrated that a well-behaved electrified anode-cathode is required to reach a well-performed corrosion inhibitor by using polarization curves instead of the gravimetric test used. It is not surprising that different kinetics behaviors is preserved if the steel surface is polarized furthest the Tafel polarization range by using anodic or cathodic potentiodynamic polarization test [53]. Thus, it requires more studies using various concentrations and types of corrosion inhibitors (or new inhibitors), temperatures, and flowing media. In this way, the studies of the cathodic, anodic, or neutral corrosion inhibitors by using a forced energy are important topics on electrochemical and corrosion research.

Table 6. CR and IE values determined from weight loss measurements of three steels exposed to OPW containing 50 mg/L CI-2 at stagnant condition after 30 days of exposure time.

Steel	Initial weight (g)	Final weight (g)	CR		IE (%)
			(mm/year)	(mpy)	
Blank					
X52	4.2610	4.2535	0.030	1.20	-
	5.9953	5.9874	0.029	1.14	-
X60	5.6686	5.6623	0.021	0.84	-
	8.4611	8.4509	0.02	0.82	-
X70	6.4013	6.3918	0.030	1.19	-
	5.2110	5.2041	0.029	1.16	-
CI-2					
X52	5.0880	5.0809	0.025	1.02	15.12
	5.0583	5.0526	0.024	0.95	17.24
X60	20.9830	20.9656	0.022	0.89	-
	24.1775	24.1512	0.028	1.1	-
X70	7.4889	7.4788	0.023	0.93	21.51
	7.6008	7.5911	0.019	0.78	34.48

Optical images of the corroded surfaces

The optical images of (a) fresh polished steels and (b) steels immersed in OPW before and after the gravimetric procedure, respectively is presented in Fig. 5. Cylindrical and cuboid geometries were used in the test with and without inhibitor. In this manner, after oxides removal on steel surfaces (Fig. 5(b)) and the CR determination by means of weight loss evaluations following in unstirred CI-2, it is possible to note that these steels had different types of surfaces discoloration related to oxide films, which were formed at stagnant situation and after 30 days of exposure time reaching a minimum surface discoloration for X70 steel with particular importance on CI-2 added. The difference between IE in both electrochemical and gravimetric testing is significative, but when the electrochemical testing was applied, a hard increased had the IE, as a consequence of the forced energy (anodic and cathodic potentials) reaching a maximum value for X70 steel (formation of an organic barrier). It may be attributed to stagnant condition and temperature in the experimental design of the gravimetric testing because a poor homogenization of the solution is highlighted. Thus, it is assumed that the low surface discoloration is attributed to evidence of a possible surface adsorbed inhibitive molecules reaching a certain surface coverage.

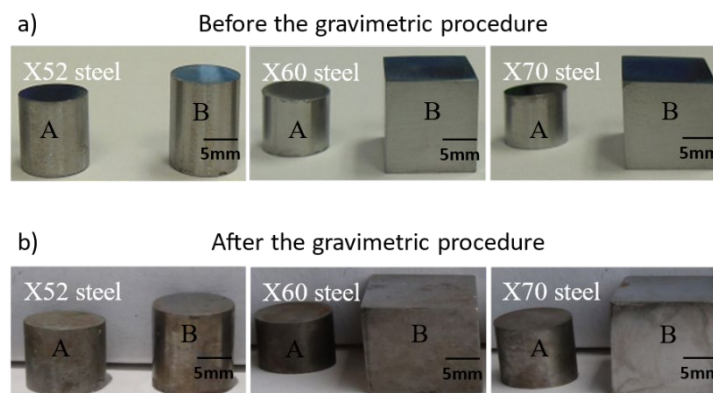


Fig. 5. Optical images of (a) fresh polished steels and (b) steels exposed to OPW at stagnant condition before and after the gravimetric procedure, respectively. Cylindrical geometries were used in the test without inhibitor and the cuboid geometries were used in the test with inhibitor.

Scanning electron microscopy images of the corroded surfaces

The SEM images of the three steels exposed to OPW after oxides removal and their CR determination by means weight loss evaluations following in unstirred CI-2 is shown in Fig. 6. Local corrosion damage for X52 and X60 steels exposed to OPW in the absence and in the presence of CI-2 was obtained, confirming that these types of steels were not well-protected activating a localized corrosion damage, where a deterioration-dissolution of possible Fe^{2+} or Fe^{3+} might happen. However, X70 steel had minor localized corrosion damage as a consequence of the well-preserved and adsorbed corrosion inhibitor to avoid the dissolution of iron compounds in the pit as was shown in X52 and X60 steels. The internal corrosion is an important technological and academic topic to consider in continuous corrosion inhibitor injection in oil and gas pipelines, and to better understand the performance of imidazoline derivatives inhibitors, it is suggested to focus more effort on well-preserved corrosion inhibitors on carbon steel pipelines considering a periodic electrochemical and gravimetric test program of commercial or new corrosion inhibitors. Fig. 7 shows a graphic image for steel corroded surfaces containing local surfaces discoloration in the absence of corrosion inhibitor where pitting corrosion or dissolution could be expected. This proposed localized corrosion (local discoloration) was based on halide compounds found in OPW (Table 1). Thus, the Fig. 7 represents a profound dissolution of Fe^{2+} in the pit from the pipe steel, where a more spread of metal dissolution and the formation of FeCl_2 is expected as a consequence of the so salty and acidic sour solution.

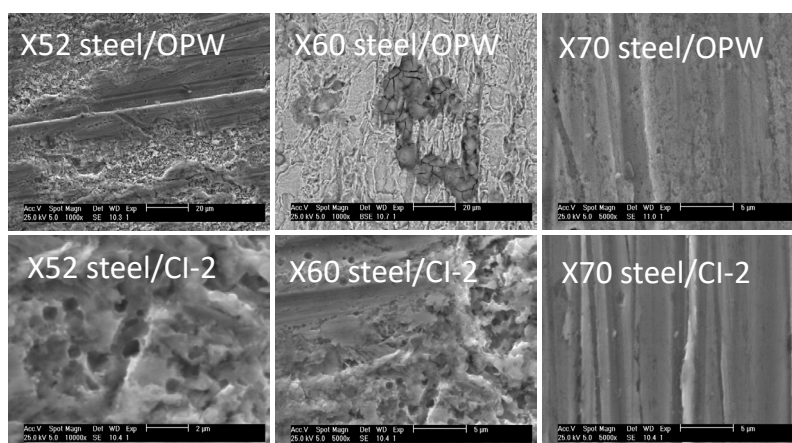


Fig. 6. SEM images of steels exposed to OPW containing CI-2 after electrochemical tests.

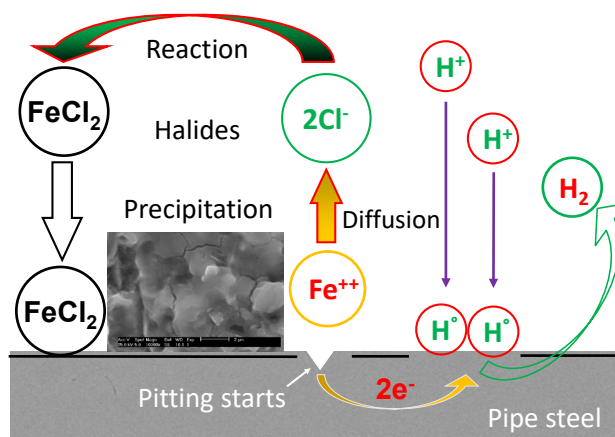


Fig. 7. Scheme for a representation of a local corrosion deterioration proposed for carbon steels exposed to OPW containing halide compounds.

Conclusions

The OPW was a corrosive medium containing a salty and acidic sour solution as a consequence of dissolved species such as halides, heavy metals, carbonates, sulfates, H₂S, and CO₂. It was naturally and electrochemically activated by flowing media, temperature in the range of 30 °C to 60 °C, and a well-behaved electrified cathode and anode from polarization curves achieving a major activity and mobility to start the deterioration of carbon pipeline steels.

Based on the Tafel slope values, a mixed corrosion inhibitor was identified by using electrochemical testing, because they remained nearly close.

Localized corrosion was obtained in the carbon steel pipelines with higher CR values in X52 and X60 steels, while X70 steel presented an apparently low generalized corrosion when it was exposed to OPW containing corrosion inhibitor (CI-2). The low corrosion rate obtained following the corrosion inhibitor added clearly indicated the presence of well-adsorbed species, which was corroborated via electrochemical, gravimetric, and scanning electron microscopy methods.

A periodic corrosion test program by using electrochemical and gravimetric methods of commercial or new corrosion inhibitors is encourage proposed at laboratory level for the reinforcement, support, or substitution of existing corrosion inhibitors in field.

In field practices, the potential advantage using corrosion coupons is that the internal corrosion rate measurements must be estimated from the same type of low carbon steel (real corrosion coupons) used in the real oil or gas pipelines in a real corrosive medium instead of commercial and nonindustrial corrosion coupons.

Acknowledgements

The authors acknowledge corrosion laboratory support from the Instituto Mexicano del Petróleo (IMP).

References

1. Groyzman, A. *Czech Assoc. Corros. Eng.* **2017**, 61, 100-117.
2. Lahme, S.; Mand, J.; Longwell, J.; Smith, R.; Enning, D. *Appl. Environ. Microbiol.* **2021**, 87, 1-17.
3. Foroulis, Z. A. *Anti-Corros. Methods Mater.* **1981**, 28, 4-9.
4. Fouda, A. S.; Elmorsi, M. A.; Fayed, T.; Shaban, S.M.; Azazy, O. *Surf. Eng. Appl. Electrochem.* **2018**, 54, 180-193.
5. Shao, Y.; Tang, J.; Zhang, T.; Meng, G.; Wang, F. *Int. J. Electrochem. Sci.* **2013**, 8, 5546-5559.
6. Álvarez-Manzano, R.; Mendoza-Canales, J.; Castillo-Cervantes, S.; Marin-Jesús, J. *J. Mex. Chem. Soc.* **2013**, 57, 30-35.
7. Garnica-Rodríguez, A.; Genesca, J.; Mendoza-Flores, J.; Duran-Romero, R. *J. Appl. Electrochem.* **2009**, 39, 1809-1819.
8. Xuejun, X.; Wanqin, Y.; Shunan, C.; Ling, P.; Xunjie, G.; Keru, P. *Anti-Corrosos. Methods Mater.* **2005**, 52, 145-147.
9. Liu, D.; Chen, Z. Y.; Guo, X. P. *Anti-Corrosos. Methods Mater.* **2008**, 55, 130-134.
10. Cheng, Y.; Bai, Y.; Li, Z.; Liu, J. G. *Anti-Corrosos. Methods Mater.* **2019**, 66, 174-187.
11. Zhou, C.; Huang, Q.; Gou, Q.; Zheng, J.; Chen, X. *Corros. Sci.* **2016**, 110, 242-252.
12. Lu, Y.; Zhang, Y.; Liu, Z.; Zhang, Y.; Wang, C.; Guo, H. *Anti-Corrosos. Methods Mater.* **2014**, 61, 166-171.
13. Zafar, M.N.; Rihan, R.; Al-Hadhrami, L. *Corros. Sci.* **2015**, 94, 275-287.

14. Demoz, A.; Papavinasam, S.; Omotoso, O.; Michaelian, K.; Revie, R. W. *Corrosion*. **2009**, *65*, 741-747.
15. Liao, K.; Yao, Q.; Wu, X.; Jia, W. *Energies*. **2012**, *5*, 3892-3907.
16. Bandyopadhyay, S.; Neogy, C.; Den, S. K. *Phys. Stat. Sol.* **1984**, *122*, 113-123.
17. Refaey, S. A. M.; Taha, F.; Abd El-Malak, A. M. *Int. J. Electrochem. Sci.* **2006**, *1*, 80-91.
18. Zarrok, H.; Zarrouk, A.; Salghi, R.; Ebn Touhami, M.; Oudda, H.; Hammouti, B.; Tourir, R.; Bentis, F.; Al-Deyab, S. S. *Int. J. Electrochem. Sci.* **2013**, *8*, 6014-6032.
19. Quej Ake, L. M.; Contreras, A.; Liu, H. B.; Alamilla, J. L.; Sosa, E. *S.E.A.E.* **2020**, *56*, 365-380.
20. Quej Ake, L. M.; Contreras, A.; Liu, H. B.; Alamilla, J. L.; Sosa, E. *Anti-Corrosos. Methods Mater.* **2018**, *65*, 281-291.
21. Quej-Aké, L. M.; Contreras, A.; Aburto, J., in: *Characterization of Metals and Alloys*, Vol. 1, Pérez Campos, R.; Contreras Cuevas, A.; Esparza Muños, R.A., Eds., Springer, Switzerland, **2017**, 13-28.
22. Quej-Aké, L. M.; Mireles, M. J.; Galvan-Martínez, R.; Contreras, A., in: *Materials Characterization*, Vol. 1, Pérez Campos, R.; Contreras Cuevas, A.; Esparza Muños, R.A., Eds., Springer, Switzerland, **2015**, 101-118.
23. Quej Ake, L.M.; Contreras, A.; Aburto, J. *Int. J. Electrochem. Sci.* **2018**, *13*, 7416-7431.
24. Bard A.J.; Faulkner, L. R. *Electrochemical Methods: Fundamentals and Applications*. J. Wiley & Sons, New York, **1980**.
25. EPA 6010C. *Inductively coupled plasma-atomic emission spectrometry (ICP-AES)*, **2000**.
26. ASTM D4327-17. *Standard Test Method for Anions in Water by Chemically Suppressed Ion Chromatography*, ASTM International, West Conshohocken, PA, **2017**.
27. Benítez, J. L.; Guzmán, G.; Muñoz L.; Sánchez, L. *O.G.J.* **2004**, *May 24*, 60-65.
28. Benítez, J. L.; Martínez, C.; Roldan, R. *O.G.J.* **2002**, *June 17*, 66-70.
29. Quej-Ake, L.M.; Marín Cruz, J.; Contreras, A. *Anti-Corrosos. Methods Mater.* **2017**, *64*, 61-68.
30. ASTM G170. *Standard Guide for Evaluating and Qualifying Oilfield and Refinery Corrosion Inhibitors in the Laboratory*, ASTM International, West Conshohocken, PA, **2012**.
31. ASTM G184. *Standard Test Method for Evaluating and Qualifying Oil and Refinery Corrosion Inhibitors Using Rotating Cage*, ASTM International, West Conshohocken, PA, **2016**.
32. ASTM G185. *Standard Test Method for Evaluating and Qualifying Oil Field and Refinery Corrosion Inhibitors Using the Rotating Cylinder Electrode*, ASTM International, West Conshohocken, PA, **2016**.
33. NACE Standard TM0177. *Laboratory Testing of Metals for Resistance to Specific Forms of Environmental Cracking in H₂S Environments*, NACE International, TX, US, **2005**.
34. Vedage, H.; Ramanarayanan, T. A.; Mumford J.D.; Smith, S. N. *Corrosion*. **1993**, *49*, 114-121.
35. ASTM G102. *Standard Practice for Calculation of Corrosion Rates and Related Information from Electrochemical Measurements*, ASTM International, West Conshohocken, PA, **2015**.
36. El Mehdi, B.; Mernari, B.; Traisnel, M.; Bentiss, F.; Lagrenée, M. *Corros. Sci.* **2002**, *77*, 489-496.
37. NACE Standard SP0775. *Preparation, Installation, Analysis, an Interpretation of Corrosion Coupons in Oilfield Operations*, NACE International, TX, US, **2018**.
38. ASTM G1-03(17). *Standard Practice for Preparing, Cleaning, and Evaluating Corrosion Test Specimens*, ASTM International, West Conshohocken, PA, **2017**.
39. NACE/ASTM TM0169. *Laboratory Corrosion Testing of Metals*, NACE International, TX, US, 2012.
40. Zhang, G. A.; Cheng, Y.F. *Corros. Sci.* **2009**, *51*, 87-94.
41. Sherif, E. S. M.; Almajid, A. A.; Khalil, A. K.; Junaedi, H.; Latief, F.H. *Int. J. Electrochem. Sci.* **2013**, 9360-9370.
42. Peng, H.; Luan, Z.; Liu, J.; Lei, Y.; Chen, J.; Deng, S.; Su, X. *Anti-Corrosos. Methods Mater.* **2021**, *68*, 438-448.
43. Quej Ake, L. M.; Contreras, A.; Lui H.; Alamilla, J. L.; Sosa, E. *Anti-Corrosos. Methods Mater.* **2019**, *66*, 101-114.
44. Quej Ake, L. M.; Contreras, A.; Aburto, J. E. *Anti-Corrosos. Methods Mater.* **2018**, *65*, 234-248.

45. Bentiss, F.; Lebrini, M.; Lagrenée, M. *Corros. Sci.* **2005**, 47, 2915-2931.
46. Negm, N. A.; Al Sabagh, A. M.; Migahed, M. A.; Abdel Bary, H. M.; El Din, H. M. *Corros. Sci.* **2010**, 52, 2122-2132.
47. Arcenegui Troya, J.; Sánchez Jiménez, P.E.; Perejón, A.; Pérez Maqueda, L. A. *J. Therm. Anal. Calorim.* **2022**. DOI: <https://doi.org/10.1007/s10973-022-11728-3>.
48. Seikh, A. H.; Sherif, E. S. M. *Int. J. Electrochem. Sci.* **2015**, 895-908.
49. Noor El-Din, M. R.; Al Sabagh, A. M.; Hegazy, E. M. A. *J. Dispersion Sci. Technol.* **2012**, 33, 1444-1451.
50. Gogoi, P. K.; Barhai, B. *Int. J. Electrochem. Sci.* **2011**, 136-145.
51. Li, S.; Zeng, Z.; Harris, M. A.; Sánchez, L. J.; Cong, H. *Frontiers in Mater.* **2019**, 6, 10. DOI: 10.3389/fmats.2019.00010.
52. Quej Ake, L. M.; García Jiménez, S.; Liu, H. B.; Alamilla, J. L.; Angeles Chavez, C. *Anti-Corrosos. Methods Mater.* **2022**, 69, 131-140.
53. ASTM G5. *Standard Reference Test Method for Making Potentiodynamic Anodic Polarization Measurements*, ASTM International, West Conshohocken, PA, **2021**.